analytical chemistry

ARTICLE

pubs.acs.org/ac

Quantitative Fluorescence Microscopy To Determine Molecular Occupancy of Phospholipid Vesicles

Emily C. Heider,[†] Eric M. Peterson,[†] Moussa Barhoum,[†] Karl-Heinz Gericke,[‡] and Joel M. Harris*[,†]

[†]Department of Chemistry, University of Utah, 315 South 1400 East, Salt Lake City, Utah 84112, United States

[‡]Institut für Physikalische and Theoretische Chemie, Technische Universität Braunschweig, 38106 Braunschweig, Germany

Supporting Information

ABSTRACT: Encapsulation of molecules in phospholipid vesicles provides unique opportunities to study chemical reactions in small volumes as well as the behavior of individual proteins, enzymes, and ribozymes in a confined region without requiring a tether to immobilize the molecule to a surface. These experiments generally depend on generating a predictable loading of vesicles with small numbers of target molecules and thus raise a significant measurement challenge, namely, to quantify molecular occupancy of vesicles at the single-molecule level. In this work, we describe an imaging experiment to measure the time-dependent fluorescence from individual dye molecules encapsulated in ~130 nm vesicles that are adhered to a glass surface. For determining a fit of the molecular occupancy data to a Poisson model, it is critical to count empty vesicles in the population since these dominate the sample when the mean occupancy is small, $\lambda \leq \sim 1$. Counting empty vesicles was accomplished by subsequently labeling all the vesicles with a lipophilic dye and reimaging the sample. By counting both the empty vesicles and those containing fluors, and quantifying the number of fluors present, we demonstrate a self-consistent Poisson distribution of molecular occupancy for well-solvated molecules, as well as anomalies due to aggregation of dye, which can arise even at very low solution concentrations. By observation of many vesicles in parallel in an image, this approach provides quantitative information about the distribution of molecular occupancy in a population of vesicles.

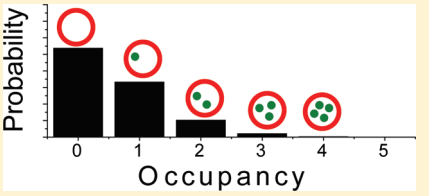

Phospholipid vesicles or liposomes are attracting considerable interest as models for biological cells,[1] as biocompatible vehicles for drug delivery,[2−5] as a means of isolating single molecules for studies of conformational dynamics,[6−8] as containers to study the reactivity of encapsulated enzymes[9,10] or other chemical reactions in small volumes initiated by vesicle fusion[11,12] or membrane phase transitions.[13] Liposomes have also been used as sensing structures in chemical analysis,[14] where, for example, the interior volume encapsulates a dye that can be released into solution upon analyte binding[15] or where analyte binding leads to a change in fluorescence of an encapsulated reporter molecule.[16] In all of these applications, there is a need for quantitative information about the population of molecules that are encapsulated within vesicles. This information is needed to characterize the loading of drugs or reporter molecules, to know the concentration of reagents in kinetics studies, or to control very small encapsulated populations for single-molecule investigations. Several recent studies have addressed the quantitative analysis of larger populations of encapsulated molecules within individual vesicles.[17,18] Sun and Chiu[17] investigated encapsulation efficiency and characterized encapsulation heterogeneity by optically trapping large (10 μm) vesicles prepared in 250 μM carboxyfluorescein; the vesicles were lysed by a UV-laser pulse, and the fluorescence from the released dye was measured to determine the interior dye concentration. More recently, Lohse et al.[18] described a fluorescence imaging method for quantifying millimolar concentrations of dye in vesicles having diameters ranging from 100 nm to 1 μm.

Quantitative analysis of very small numbers of molecules in individual vesicles poses a greater challenge. Encapsulation of single biomolecules has enabled the study of the single-molecule dynamics of ribozyme[7] and protein[8] folding and protein−DNA[19] interactions. Ensuring that only single molecules are encapsulated requires control over the size of the vesicles, concentration of the target analyte and interactions of the analyte with the phospholipid membrane.[20] When the average number of encapsulated molecules is small, the occupancy of individual vesicles is expected to follow a Poisson distribution, if the vesicle volumes are uniform and the encapsulated molecules do not interact with each other or the vesicle membrane. Control over the size of the vesicles[21−24] is also critical to achieving a predictable distribution of molecular occupancy.

Several methods have been developed to assess encapsulation at the limit of a few molecules per vesicle. Vesicles incorporating biotinylated lipids in their membranes have been attached via a streptavidin linker to biotinylated lipid bilayers deposited on glass surfaces; the fluorescence of labeled molecules was imaged, and discrete photobleaching steps were counted to determine the vesicle occupancy.[6,7] The sample preparation used in this method for vesicle immobilization is tedious, unencapsulated molecules are not detected, and empty vesicles are not counted. To address some of these limitations, Reiner et al.[25] recently

Received: January 17, 2011
Accepted: May 23, 2011
Published: June 07, 2011

reported using fluorescence correlation spectroscopy (FCS) to measure dye encapsulation. They were able to distinguish free-solution (unencapsulated) dye molecules from those entrapped in small (<100 nm) vesicles, employing FCS to discriminate these two populations based on their characteristic diffusion in solution. From the relative amplitude of these two populations versus dye concentration, the encapsulation efficiency could be determined in a nondestructive manner. They utilized a Poisson occupancy model to reveal the significant influence of the variation in dye brightness on the autocorrelation analysis[25] which had been neglected in previous FCS studies.[26,27] In addition, the size distribution of vesicles was determined by field-flow fractionation combined with multiple-angle laser light scattering so that its effect on the reported encapsulation efficiency could be assessed.[25]

Immobilized vesicle imaging and FCS are both useful methods to observe encapsulation near the single-molecule limit. Nevertheless, neither method characterizes the population of empty vesicles, which can be considerable and even dominant when the average occupancy is on the order of one molecule or less. In this work, a simple method of vesicle immobilization on clean glass surface is combined with imaging by epi-illumination fluorescence microscopy to measure the intensity of encapsulated dye molecules within the vesicles over time. Counting the number of photobleaching steps for each vesicle in the image over time allows determination of the occupancy of a large population of vesicles in parallel. A unique aspect of this work is the goal of counting empty vesicles in the sample, where a lipid-soluble dye, Nile red, is added to the solution to label all the vesicles in an image. The fluorescence of Nile red is sensitive to polarity, exhibiting a large increase in quantum yield in hydrophobic environments, with very low emission in aqueous solution.[28,29] Nile red will label both the occupied and unoccupied vesicles so that the total number of vesicles present in an image can be counted, providing a complete distribution of molecular occupancy in the vesicle population. The possibility of measuring the fluorescence intensity of vesicles to quantify the number of encapsulated fluors was also tested, and problems arising from aggregation of the dye and its intensity variation were investigated.

EXPERIMENTAL SECTION

Reagents and Materials. 1,2-Dipalmitoyl-*sn*-glycero-3-phosphocholine (DPPC) and a miniextruder apparatus were acquired from Avanti Polar Lipids, Inc. (Alabaster, AL). Polycarbonate membranes for the extruder were purchased from Nucleopore (Pleasanton, CA). Spectrophotometric-grade dimethylformamide (DMF), methanol, and ethanol were obtained from Fisher Scientific (Hampton, NH). Chloroform, $Na_2HPO_4 \cdot H_2O$, and NaOH were from Mallinckrodt (Paris, KY). Dyes were purchased from a variety of sources: laser-grade sulforhodamine B (SFRB, from Sigma-Aldrich, St. Louis, MO), Cy3 and Cy3B mono NHS ester (GE Healthcare, Buckinghamshire, U.K.), Oyster 550 NHS ester (Denovo Biolabels, Münster, Germany), and Nile red (Invitrogen Corporation, Carlsbad CA). The buffer (40 mM phosphate pH 7.4) was prepared from quartz-distilled water that was filtered using a Barnstead NANOpure II filter (Boston, MA) to a 18 MΩ·cm resistivity. The buffer solution was filtered with 0.2 μm filters from Fisher Scientific (Santa Clara, CA). Glass coverslips (no. 1, 22 × 22 mm^2) were acquired from VWR (West Chester, PA) and cleaned by rinsing in methanol before being UV−ozone (UVO)-cleaned for 25 min per side (Jelight Co. model 342).

Sample Preparation. The DPPC lipid film was prepared by evaporating the chloroform from 200 μL of lipid solution containing 5 mg/mL DPPC under nitrogen, and then the film was subjected to vacuum for 2 h. The lipid films were hydrated initially with 1 mL of buffer containing 0.5−5 μM SFRB. Later, the vesicle hydration solution was modified (as discussed below) to comprise 90:10 (vol %) buffer/DMF containing 0.5−5.0 μM SFRB. The hydrated vesicles were further treated according to the procedure described by Mayer et al.[22] in which the dispersion was repeatedly freeze−thaw treated, prior to extrusion through two stacked membranes. The hydrated lipid was freeze−thaw cycled five times between liquid nitrogen and a 64 °C water bath, 10 min for each step. The vesicles were then stored in the water bath between 1 and 5 h prior to extrusion through two-stacked 100 nm pore membranes; each sample was imaged before the next was extruded.

For dynamic light scattering (DLS) experiments, the extruded vesicle dispersion was diluted 100 μL into 3 mL of buffer. For fluorescence imaging, the extruded vesicles were diluted 25 μL to 5 mL of buffer. To obtain low vesicle densities on the surface, the extruded vesicle solution was further diluted, adding 50 μL of the vesicle solution to 2 mL of buffer in the imaging well (a glass cylinder epoxy-adhered to the glass coverslide). It has been shown[30] that vesicles having gel-phase phosphatidylcholine membranes adhere to clean glass without rupture or fusion, a characteristic exploited here to observe the same population of immobilized vesicles in parallel over time. To remove free dye from the overlaying solution, 2 mL of buffer was exchanged in the well cell a minimum of five times, resulting in a concentration of free SFRB of ∼20 pM. The vesicles adsorbed to the glass surface were imaged with continuous illumination using the epi-illumination microscope described below. After the SFRB had photobleached, Nile red in phosphate buffer was pipetted into the well cell to a final concentration of 20 nM. The Nile red partitions into the membrane, allowing all of the vesicles adhered to the glass surface to be imaged.

Dynamic Light Scattering Measurements. A commercial NICOMP submicrometer particle sizer (Particle Sizing Systems, Santa Barbara, CA) was used to measure the size of the vesicles produced by extrusion. Light scattering of 639 nm beam at 25 °C in buffer (viscosity 0.894 cP) was used to measure diffusion of the vesicles and determine their number-weighted size distribution.

Fluorescence Microscopy. Images were collected using an epi-illumination fluorescence microscope. The emission beam from a 532 nm diode laser (B&W Tek Inc.) was circularly polarized with a $\lambda/4$ waveplate and coupled into polarization-maintaining optical fiber. The excitation light from the fiber was passed through a filter cube containing an excitation filter (FF01-531/22-05, Semrock) and dichroic beam splitter (FF555-DiO2-25×36) and through an Olympus 60×, 1.45 N.A. oil-immersion objective to illuminate vesicles adhered to the surface of a coverslip. The fluorescence emission was collected by the same objective and passed through the cube containing an emission filter (FF01-582/75-25) and imaged onto the detector, a Photometrics EMCCD detector (Cascade II 512, Photometrics). Metamorph Imaging software (Universal Imaging) controlled the EMCCD. Vesicles were imaged with 100 ms integration times for 1000 frames (100 s movies) to observe the photobleaching time profile.

Image Analysis. The images of vesicles with encapsulated SFRB and of Nile red-labeled vesicles were processed to determine their intensities as a function of time. The in-house Matlab (Mathworks) program used for fitting the background and locating spots in the image has been described previously.[31] Briefly, a moving average background from five sequential images was subtracted from each image, and spots were identified with the criterion of three adjacent pixels displaying an intensity 2.5 times the standard deviation of the background. Once the spot was identified, then the intensities of all the pixels within a three pixel radius were summed to determine the total intensity of the vesicle. The intensity of a given spot was calculated for each image in the 1000-frame movie.

To evaluate the limits of sizing vesicles in the images, the point spread function (PSF) of the fluorescence microscope was measured by imaging the fluorescence of single SFRB molecules deposited onto a glass coverslip by a substrate withdrawal method.[32,33] Briefly, a glass coverslip was rinsed with methanol, dried, and placed in a UVO cleaner for 25 min per side. The clean coverslip was withdrawn from an 80 pM solution of SFRB in methanol at a constant velocity of 1.5 cm/s. Dye deposited on one side of the glass was removed by rinsing with copious quantities of methanol, and the opposite side then was imaged with the epi-illumination microscope (see Figure S1 in the Supporting Information). Using a two-dimensional (2D) Gaussian fit of the data, the PSF was measured to have a full width at half-maximum (fwhm) of 360 nm, which was larger than the predicted diffraction-limited spot size, fwhm = 0.61λ/N.A. = 260 nm, for the 1.45 N.A. objective and emission maximum of 610 nm.[34] This discrepancy arises from the significant pixel size of the CCD, which in the object plane is 270 nm, close to the diffraction-limited spot size. When convoluted together, these two sources of spatial uncertainty should produce a PSF that is $\sim\sqrt{2}$ larger than the individual contributions,[35] which is very close to the observed PSF result.

Control Experiments. To test whether residual SFRB dye from solution would adsorb to the clean glass surface and interfere with the analysis of vesicles, a solution of the 5.0 μM dye was diluted using the same volumes as the vesicle-containing samples and then added to a well cell, following which, the buffer was exchanged as above. The surface was imaged, and no fluorescent spots could be detected. Similarly, 20 nM Nile red in buffer was added to a well cell and imaged with no vesicles present, and no fluorescent spots could be observed (Figure S2 in the Supporting Information).

It has been demonstrated[36] that vesicles above their transition temperature adhering to glass can fuse to the surface and form a supported lipid bilayer, which would cause their contents to escape and would lead to erroneous encapsulation results. While vesicle fusion rates are much slower at temperatures below the membrane phase transition[37] and, therefore, not expected to interfere with the present results, a control experiment was conducted to determine whether the loss of intensity from vesicles over time was due to vesicle fusion and release of contents, rather than photobleaching, as discussed below. For this experiment, DPPC vesicles containing 2.5 μM SFRB were dispersed onto the glass coverslide and imaged intermittently (100 ms every 5 min) rather than continuously. After 15 min, SFRB is clearly still retained in all the vesicles present on the surface (see Supporting Information Figure S3), which demonstrates that the membranes of the adhered vesicles are sufficiently stable to provide encapsulation over a 24-fold longer time than is needed to observe entrapped SFRB photobleaching.

Counting empty vesicles is accomplished by labeling all the vesicles present with Nile red after the encapsulated SFRB had been photobleached for periods longer than 100 s. To be certain that the SFRB was fully photobleached before the addition of Nile red to label the entire vesicle population, the photobleaching decay time was determined by monitoring the total intensity from 0.5 μM SFRB encapsulated in vesicles over 100 s. The decay curve of the total intensity fit a single-exponential decay with $\tau = 17.9 \pm 0.3$ s (see Supporting Information Figure S4A). On the basis of these results, the fraction of SFRB that would remain unbleached after 100 s of illumination is $\exp(-100/17.9)$ or 0.0037. Additionally, a histogram of the time required for single-molecule photobleaching was scrutinized to evaluate the possibility that two molecules could photobleach during a single 100 ms integration time (see Supporting Information Figure S4B). The histogram also fit a single-exponential, with average time to photobleach of 18 s. The area under the normalized histogram between 0 and 100 ms (the integration time) gives the probability of a single photobleaching event occurring of 5.5×10^{-3}. Therefore, the probability of two events occurring in the same 100 ms interval is the single-event probability squared, or 3×10^{-5}. Thus, it is very improbable that a reported photobleaching step corresponds to two photobleaching events.

RESULTS AND DISCUSSION

Encapsulation of Individual Molecules in Vesicles. The occupancy of fluorescent SFRB molecules in phospholipid vesicles can be monitored by observing the stepwise photobleaching of the fluors entrapped in the aqueous interior of the vesicle. The dye (SFRB) was selected for its water solubility arising from two sulfonate groups and a quaternary amine, and because SFRB was reported not to interact with phospholipid membranes.[25] For vesicles containing a single dye molecule, it is expected that the illuminated fluor would produce an emission signal until it undergoes photobleaching, which would be recorded in an intensity versus time trace as a single-step decrease in intensity to the baseline.[6,7] In initial experiments, vesicles were loaded with SFRB that was prepared in a purely aqueous buffer. The fluorescence of these vesicles showed a very wide range of intensities, even for the lowest dye concentrations, where the vesicles were expected to contain only a few fluors. As shown in Figure 1, parts A and B, vesicle intensities ranged over nearly 2 orders of magnitudes. Examination of the photobleaching traces (Figure 2, parts A and B) showed that the less intense spots from the images usually exhibited only one or two photobleaching steps (averaging ~650 counts each), whereas the brighter spots show as much as 30 times this initial intensity and tens of photobleaching steps. This behavior suggests that, despite the water solubility of SFRB, the dye is aggregating and is not entirely dissolved as individual molecules when prepared at micromolar concentrations in aqueous solution.

Aggregation clearly interferes with any quantitative interpretation of vesicle encapsulation of single molecules. To address this problem, several alternative strategies for sample preparation were tested. The first involved dissolving the solid SFRB in organic solvents ethanol or DMF at millimolar concentrations followed by dilution in aqueous buffer to prepare the desired micromolar concentrations of SFRB for vesicle encapsulation. These conditions were not successful in avoiding aggregation and yielded results similar to those observed for SFRB dissolved directly in buffer (example photobleaching traces of vesicles from

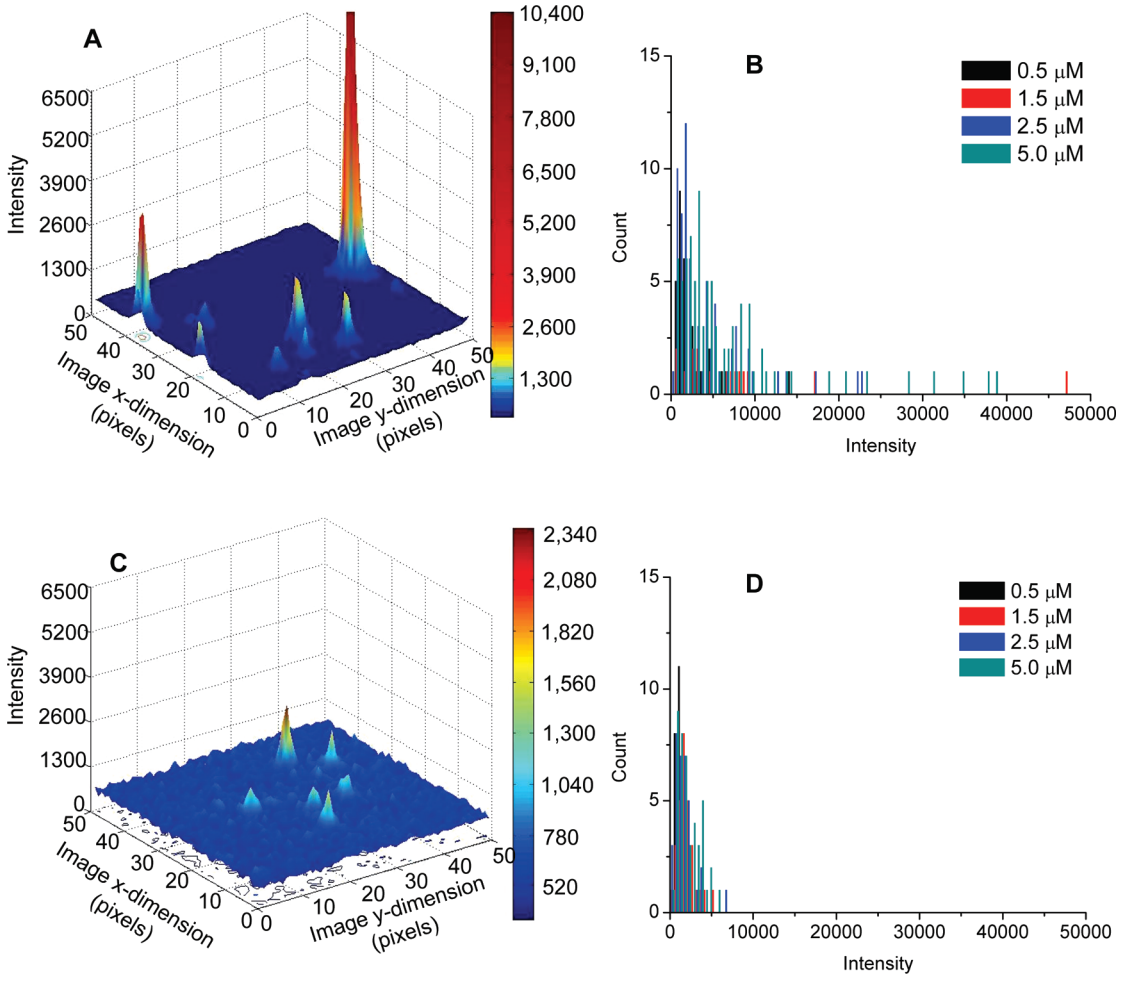

Figure 1. Fluorescence intensity variation of SFRB-containing vesicles. (A and B) In DPPC vesicles hydrated and extruded in aqueous buffer, aggregation is apparent in the significant variation in intensities. (A) Three-dimensional projection of an image of vesicles encapsulating 2.5 μM SFRB in buffer. (B) Histogram of intensities for four different dye concentrations. (C and D) Vesicles hydrated and extruded in a solution containing SFRB in 10% DMF−90% phosphate buffer show significantly less aggregation. (C) The 3D projection of an image of vesicles containing 2.5 μM SFRB with this preparation show more uniform intensity, also apparent in panel D, the histogram of intensities for four different dye concentrations.

these samples are included in the Supporting Information). Finally, a strategy was tested where the dye was dissolved and initial millimolar solutions prepared in 100% DMF, followed by dilution into aqueous buffer that included 10% DMF, and these solutions were then used for hydrating the lipid and extruding vesicles. After the vesicles were extruded in 10% DMF solution and encapsulation was complete, the vesicles were diluted into purely aqueous buffer, and furthermore, the buffer used in the solvent exchange step to remove the free dye also did not contain DMF. This procedure yielded a dispersion of SFRB as single molecules without dye aggregates encapsulated in the vesicles. This is clearly evident in the distribution of intensities shown in Figure 1, parts C and D, where the outlier intensities are gone and the increase in the intensity tracks the dye concentration of the entrapped solution. Even with 10% DMF in hydrating solution, the resulting vesicles and their contents were stable over the time required to measure the intensities and complete the experiment (hours). Since the presence of DMF was required to ensure encapsulation of individual SFRB molecules in vesicles, all measurements of the SFRB intensities and photobleaching were acquired with DMF in solution.

Measuring Molecular Occupancy of Individual Vesicles. With the use of fluorescence imaging to measure the time history of emission from a collection of surface-attached vesicles, the numbers of SFRB photobleaching steps were measured and used to quantify the number of dye molecules present in the vesicles. Example SFRB emission traces and a plot of their initial intensity versus the number of photobleaching steps are shown in Figure 3. The linear relationship between the initial fluorescence intensity of a vesicle and the number of photobleaching steps indicates that the dye molecules are emitting independently, producing a signal which adds, on average, 630 $\pm$ 10 counts to the intensity in the first 100 ms of observation prior to photobleaching. Once the photobleaching of the encapsulated SFRB was recorded, Nile red was added to illuminate all the vesicles present, allowing counting of all vesicles including those that had not contained any SFRB molecules. Example images of the vesicles prepared at low concentrations of SFRB acquired before and after the addition of Nile red are shown in Figure 4.

Having determined the number of molecules in each vesicle as well as the number of empty vesicles, the resulting occupancy

dx.doi.org/10.1021/ac200129n |*Anal. Chem.* 2011, 83, 5128–5136

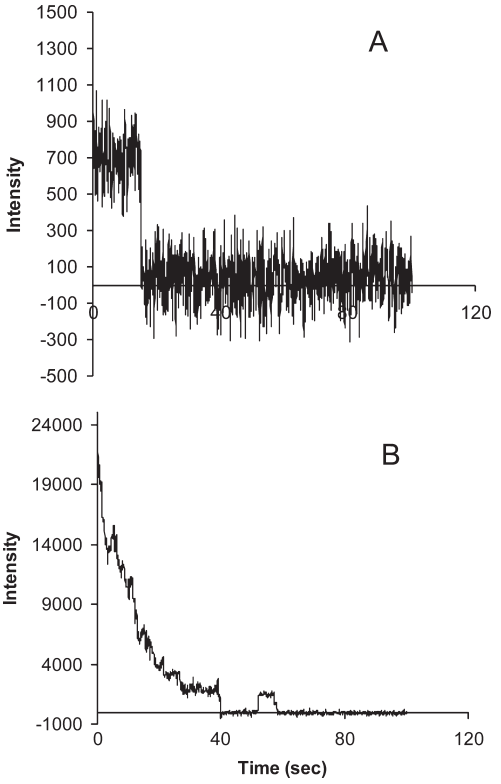

Figure 2. Photobleaching transients for SFRB encapsulated in DPPC vesicles hydrated and extruded in aqueous buffer. (A) Example fluorescence trace for a low-intensity vesicle, showing the bleaching of a single SFRB molecule. (B) A fluorescence trace for a high-intensity vesicle, where tens of SFRB molecules are bleached, showing evidence of dye aggregation.

distributions can be compared with a fit to a Poisson distribution,[38] which assumes that the molecules are drawn from a large population in the hydrating solution, where the probability of encapsulation is small due to the small volume of individual vesicles. The Poisson probability, P, for a given molecular occupancy, n, is given by[38]

$$P = \frac{\lambda^n e^{-\lambda}}{n!} \quad (1)$$

where the average number of molecules per vesicle is given by the Poisson mean, λ. This equation was fit to the molecular occupancy data for five different concentrations of dye in the hydrating solution, and the results are plotted in Figure 5 where the best-fit values of the Poisson mean are also listed in Table 1. The occupancy results are well-described by Poisson distributions, where the need for measuring the fraction of unoccupied vesicles is clear when the mean of the distribution, λ, is less than unity, and unoccupied vesicles dominate the distribution.

The molecular occupancy results can be compared to the expected values based on the vesicle volumes and the concentration of dye in the original lipid hydrating solution. If the encapsulation efficiency is unity, reflecting an unbiased sample of the hydrating solution dye concentration, then the average occupancy, λ, should be given by the product of the vesicle volume, V, in liters, the molar concentration of dye, C, and

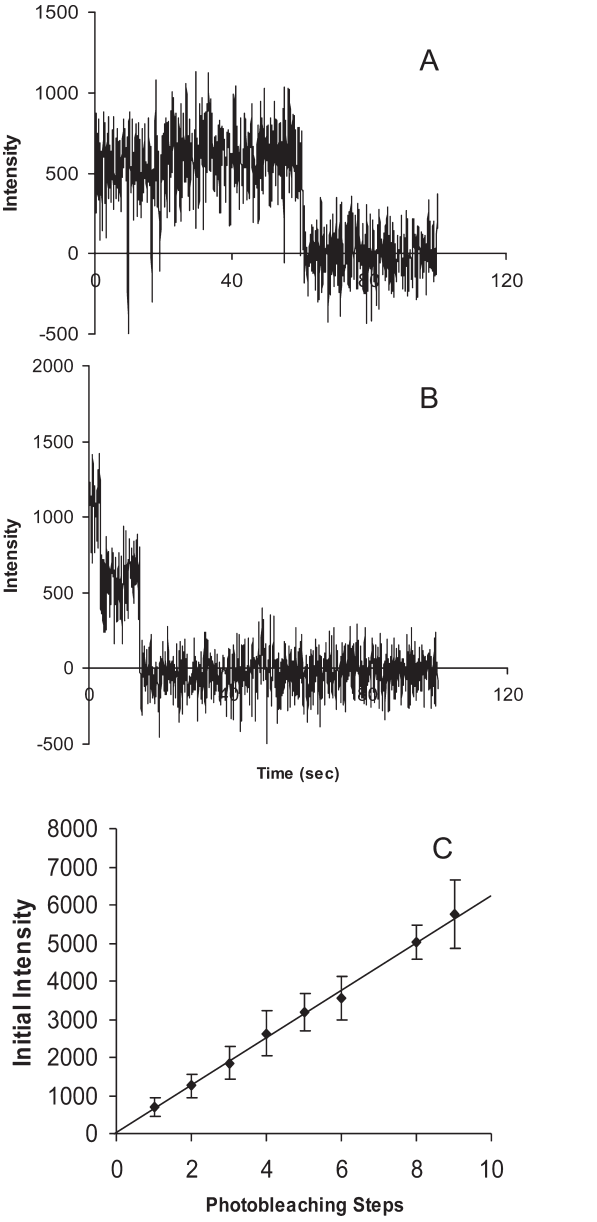

Figure 3. Photobleaching of SFRB encapsulated in DPPC vesicles hydrated and extruded in 10% DMF−90% phosphate buffer. (A and B) Example photobleaching traces showing a vesicle containing one SFRB molecule (A) and a vesicle containing two SFRB molecules (B). (C) The initial fluorescence intensity of vesicles plotted vs the number of photobleaching steps, with the results fit to a straight line with a slope of 630 ± 10 counts per molecule.

Avogadro's number, N_A:

$$\lambda = VCN_A \quad (2)$$

On the basis of the measured occupancy results in Table 1, this equation was used to solve for the predicted vesicle volume in liters and converted to an equivalent vesicle diameter. These results are listed in Table 1 and compared with the measured vesicle sizes.

The average sizes of the vesicles in solution were measured by DLS and are also listed in Table 1. It is clear from these results that the optical resolution of fluorescence imaging (360 nm fwhm PSF from single-molecule images, see the Supporting

dx.doi.org/10.1021/ac200129n |*Anal. Chem.* 2011, 83, 5128–5136

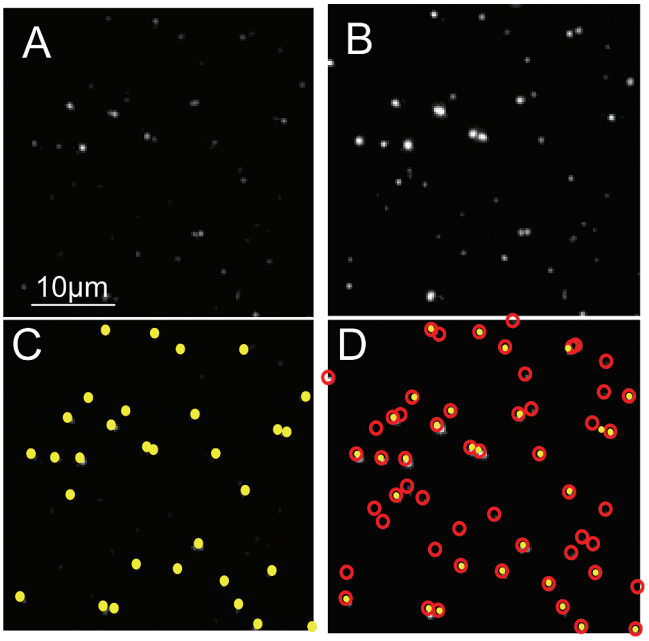

Figure 4. Fluorescence images of vesicles before and after addition of Nile red: (A) encapsulated 1.5 μM SFRB; (B) after SFRB photobleaching, Nile red is added to vesicles in panel A; (C) locations of vesicles in panel A are shown with yellow points; (D) after SFRB photobleaching, locations of vesicles labeled with Nile red are shown as red circles. Nile red staining allows the number of vesicles that do not contain SFRB molecules to be counted.

Information) is inadequate to determine the sizes of individual vesicles, which are less than half the measured PSF. The DLS results revealed a small difference in the average sizes of the extruded vesicles, which varied with the length of time that the lipid suspensions were stored in the hydrating solution prior to extrusion; Table 1 shows the vesicle sizes reported from DLS and the Poisson fit. Because the suspensions were stored at a temperature above the lipid phase transition, the smaller vesicles produced after longer times (which also coincided with the vesicles prepared at higher SFRB concentrations) likely arose from the thermal disruption of multilamellar lipid aggregates leading to smaller, more uniform vesicles upon extrusion.

Despite this variation in average vesicles size, the DLS results agree well with the vesicle sizes determined from the Poisson mean occupancy, λ, and the average vesicle volume found through eq 2; see Table 1. Even the trend in average vesicle size between samples is reproduced by the Poisson occupancy results. Thus, the average DLS vesicle sizes are consistent with the Poisson molecular occupancy results under the assumption that the encapsulation efficiency is unity. The uncertainty in the DLS measured sizes is, however, quite large (~25%), which prevents precise determination of encapsulation efficiency. If the sizes of the vesicles were more precisely measured, the encapsulation efficiency could be more critically evaluated.

As discussed in the introduction, a method has been previously reported[25] for predicting vesicle occupancy using FCS to measure unencapsulated versus encapsulated dye. FCS analysis provides a precise measurement of a vesicle size distribution, in contrast to the method described here for which the sizes are not as well-characterized. Despite the superior measurement of vesicle size, the FCS measurements cannot detect unoccupied vesicles and have indicated an encapsulation efficiency of only 30%, which is difficult to rationalize unless dye is somehow excluded from the solution within the vesicle interior. In the present work where both occupied and unoccupied vesicles were counted, the occupancy results are consistent with a Poisson statistical model assuming 100% encapsulation efficiency.

Fluorescence Intensity as a Measure of Number of Molecules. Although counting photobleaching steps to determine vesicle occupancy is quite effective, it would greatly simplify the experiment if occupancy could be predicted directly from a measurement of the initial fluorescence intensity of dye molecules contained within a vesicle. This measurement would require only a single image to evaluate the fluorescence emission rather than a series of images in succession to count the number of photobleaching steps. The linear correlation between the average initial intensity and the number of fluors (see Figure 3) suggests the feasibility of this approach. To test this possibility, the measured initial fluorescence intensities for individual vesicles were separated into populations by the number of photobleaching steps, and histograms of the intensities were plotted; see Figure 6. The results show the limitation of intensity measurements for estimating molecular numbers due to the large variation in intensities of individual molecules. Since the distribution of initial fluorescence intensities for the single-step photobleaching population overlaps the initial intensities for two photobleaching events, any attempt to quantify the number of fluors based solely on initial intensity would result in erroneous occupancy assignments, even with very low concentrations of fluors. The situation becomes worse as the number of molecules in a vesicle increases, because the variances of the individual molecule intensities are added and lead to greater uncertainty in the total signal. One approach to dealing with single-molecule intensity variations is through modeling of the intensity distribution,[39] which has been applied in estimating the number of proteins in synaptic vesicles.[40]

There are several potential sources of intensity variation, the simplest of which would be differences in intensity of excitation, which would depend on the uniformity of illumination of the sample by the microscope. In this case, the variation in fluorescence background between extreme regions of the image was only 5%, which is equivalent to the standard deviation between adjacent pixels. Additionally, some traces of two molecules trapped in the same vesicle show large variation in intensity for each photobleaching step, despite their being located at the same point in the excitation field. The polarization of the excitation can produce intensity variation for stationary molecules, but the illumination in this case was circularly polarized and the rapid rotational motion of the buffer-soluble dye molecules within a vesicle would preclude intensity variation arising from alignment of the fixed fluors relative to the excitation polarization.

Studies of single fluors in polymers,[41,42] membranes,[29] and adsorbed to surfaces[43,44] have noted intensity fluctuation linked to spectral diffusion,[41,43] photoblinking,[41] and interactions with the surrounding dielectric material.[29,45] If the variation in intensity for single fluorescent molecules were attributable to rapid (~1 ms) triplet-state photoblinking,[41] the resulting intensity fluctuations would be averaged over the 100 ms integration times. Since spectral diffusion has only been reported to occur within solids or on solid surfaces, it is unlikely that this phenomenon would significantly contribute to intensity variation of soluble molecules encapsulated in liquid solutions inside of vesicles. Another characteristic of dye fluorescence behavior that would inhibit

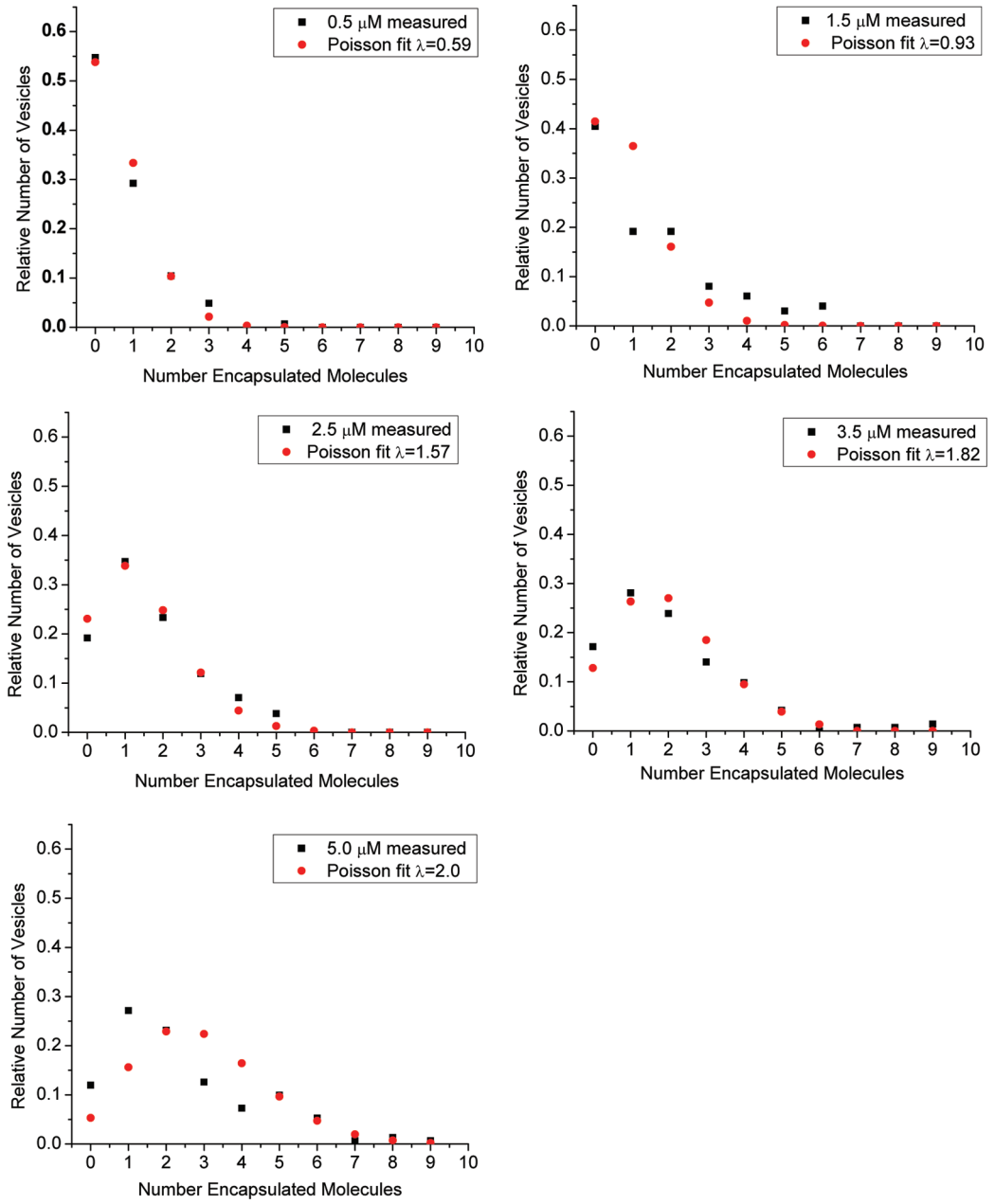

Figure 5. Histogram of SFRB molecular occupancy in DPPC vesicles determined from photobleaching traces of the encapsulated SFRB followed by counting all vesicles after staining with Nile red. The fractions of vesicles containing a given number of fluors are plotted for each concentration of SFRB (black squares), with fits to Poisson probability distributions (red circles) also shown.

Table 1. Vesicle Sizes Calculated from the Fit of the Occupancy Data to a Poisson Distribution and Measured by Dynamic Light Scattering

[SFRB] (μM)	fitted Poisson mean (λ)	diameter of vesicles (nm, Poisson fit)	diameter of vesicles (nm, from DLS)
0.5	0.59 ± 0.03	155 ± 1	160 ± 40
1.5	0.93 ± 0.15	126 ± 1	123 ± 30
2.5	1.57 ± 0.06	126 ± 1	123 ± 30
3.5	1.82 ± 0.07	118 ± 1	130 ± 32
5.0	2.00 ± 0.16	108 ± 1	130 ± 32

molecular counting by initial intensity measurements is long-lived photoblinking. This phenomenon has been observed by others in the study of single molecules on surfaces.[43,44] A sizable fraction (~30%) of the photobleaching traces of SFRB exhibit photoblinking (recovery of fluorescence after loss) on a time scale longer than the 100 ms image acquisition time (see examples in Figure 7). If one or more of these photoblinking events occurs during the acquisition of the initial image, a reported occupancy based on an initial intensity measurement would clearly be in error.

To determine whether a broad distribution of single-molecule intensities was unique to SFRB, other dyes were encapsulated in DPPC vesicles and their photobleaching behavior examined.

dx.doi.org/10.1021/ac200129n |*Anal. Chem.* 2011, 83, 5128–5136

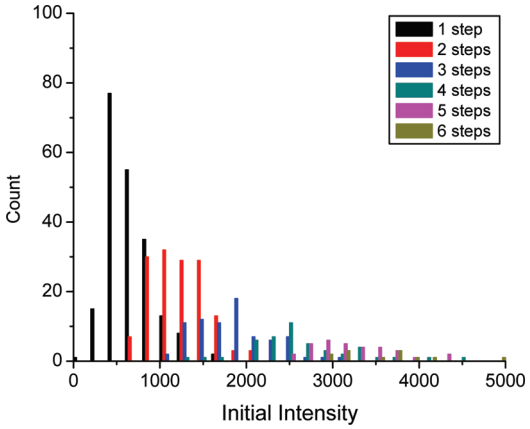

Figure 6. Histogram of initial fluorescence emission intensities for a given number of photobleaching steps. The distributions of initial fluorescence intensities for vesicles containing different numbers of molecules overlap each other and preclude quantification of the number of fluors using intensity alone.

Commonly used fluorescent labels Cy3, Cy3b, and Oyster 550 were also vesicle-encapsulated and tested, and the intensities of the individual fluors as a function of time were measured. Photobleaching traces from these dyes all exhibited intensity characteristics similar to that of SFRB, for which initial intensities for single molecules varied widely and photoblinking behavior was observed. Although this is not a comprehensive survey of fluorescent labels, it is apparent that single-molecule counting based on intensity measurements is challenging and should be interpreted only after additional evaluation of the photobleaching and photoblinking behavior of the dye.

Conclusions. This study reports a fluorescence imaging method to characterize the distribution of molecular occupancy in individual phospholipid vesicles at the single-molecule limit, including the counting of vesicles that contained no encapsulated fluors. Counting empty vesicles was accomplished by Nile red staining of all vesicles after photobleaching of the encapsulated dye. An initial obstacle to this method was the aggregation of the SFRB dye at micromolar concentrations prepared in aqueous solutions. Vesicle encapsulation, followed by fluorescence imaging, is uniquely suited to investigating molecular aggregation down to the limit of isolated free molecules. For SFRB, aggregation was eventually prevented by including 10% DMF in the dye solution used to hydrate the lipid films and extrude the vesicles. The DPPC vesicles prepared under these conditions were stable well beyond the duration of the experiment, and photobleaching traces of the dye were acquired without interference due to surface-adsorbed dye or vesicle membrane rupture. By counting photobleaching steps in dye-occupied vesicles, followed by Nile red staining to count empty vesicles, the resulting distribution of occupancies could be fit a Poisson distribution model, and the results were consistent with unit encapsulation efficiency. It was also observed that the variation in the intensities of fluorescence emitted by individual fluors, which appears to derive from long-lived photoblinking, may hinder efforts to quantify molecular occupancy in vesicles based on intensity alone.

A limitation of the present method in reporting encapsulation efficiency was the inability to accurately determine the size of individual vesicles. Dynamic light scattering reported average vesicle diameters with ~25% uncertainty, which severely restricts our ability to report encapsulation efficiency. Because extrusion generally produces a vesicle population with size variation,[46]

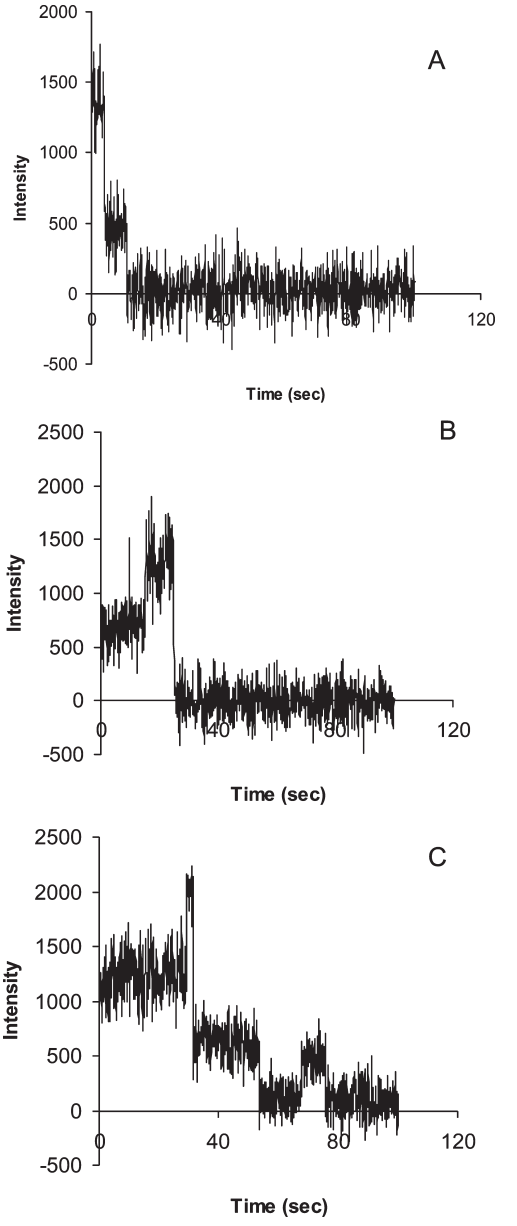

Figure 7. Photobleaching traces of SFRB encapsulated in vesicles showing (A) variation in intensity between single fluors enclosed in the same vesicles and (B and C) long-lived (seconds) "on−off" states.

it would ideal to combine the sizing of individual vesicles with determining their corresponding molecular occupancy. To conduct a size-selective analysis on an individual vesicle basis, the optical resolution of this experiment would need to be improved, which might be accomplished using methods such as subdiffraction limit microscopy.[47] This approach has been applied successfully to single-molecule imaging of Nile red in lipid bilayers[48] and could be adapted to the secondary imaging step to combine molecular occupancy with subdiffraction vesicle sizing.

■ ASSOCIATED CONTENT

Supporting Information. Additional information as noted in text. This material is available free of charge via the Internet at http://pubs.acs.org.

AUTHOR INFORMATION

Corresponding Author
*E-mail: harrisj@chem.utah.edu.

ACKNOWLEDGMENT

We appreciate the assistance of Eric Brozek and Nathan Walton in the Zharov research group at the University of Utah in the acquisition of dynamic light scattering data. This research was supported in part by the National Science Foundation under Grant CHE-0957242; additional support from the U.S. Department of Energy for image processing contributions is also acknowledged.

REFERENCES

(1) Torchilin, V.; Weissig, V. *Liposomes, A Practical Approach*, 2nd ed.; Oxford University Press: Oxford, U.K., 2003.
(2) Drummond, D. C.; Zignani, M.; Leroux, J.-C. *Prog. Lipid Res.* **2000**, *39*, 409–460.
(3) Medina, O. P.; Zhu, Y.; Kairemo, K. *Curr. Pharm. Des.* **2004**, *10*, 2981–2989.
(4) Wang, G. In *Drug Delivery, Principles and Applications*; Wang, B., Siahaan, T. J., Soltero, R. A., Eds.; John Wiley: Hoboken, NJ, 2005.
(5) Samad, A.; Sultana, Y.; Aqil, M. *Curr. Drug Delivery* **2007**, *4*, 297–305.
(6) Boukobza, E.; Sonnenfeld, A.; Haran, G. *J. Phys. Chem. B* **2001**, *105*, 12165–12170.
(7) Okumus, B.; Wilson, T. J.; Lilley, D. M.; Ha, T. *Biophys. J.* **2004**, *87*, 2798–2806.
(8) Rhoades, E.; Cohen, M.; Schuler, B.; Haran, G. *J. Am. Chem. Soc.* **2004**, *126*, 14686–14687.
(9) Chiu, D. T.; Wilson, C. F.; Karlsson, A.; Danielsson, A.; Lundqvist, A.; Strömberg, A.; Ryttsén, F.; Davidson, M.; Nordholm, S.; Orwar, O.; Zare, R. N. *Chem. Phys.* **1999**, *247*, 133–139.
(10) Cheng, Z.; D'Ambruos, G. D.; Aspinwall, C. A. *Langmuir* **2006**, *22*, 9507–9511.
(11) Chiu, D. T.; Wilson, C. F.; Ryttsen, F.; Stromberg, A.; Farre, C.; Karlsson, A.; Nordholm, S.; Gaggar, A.; Modi, B. P.; Moscho, A.; Garza-Lopez, R. A.; Orwar, O.; Zare, R. N. *Science* **1999**, *283*, 1892–1895.
(12) Kulin, S.; Kishore, R.; Helmerson, K.; Locascio, L. *Langmuir* **2003**, *19*, 8206–8210.
(13) Bolinger, P.-Y.; Stamou, D.; Vogel, H. *J. Am. Chem. Soc.* **2004**, *126*, 8594–8595.
(14) Edwards, K. A.; Baeumner, A. J. *Talanta* **2006**, *68*, 1421–1431.
(15) Ishimori, Y.; Rokugawa, K. *Clin. Chem.* **1993**, *39*, 1439–1443.
(16) Nguyen, T.; Rosenzweig, Z. *Anal. Bioanal. Chem.* **2002**, *374*, 69–74.
(17) Sun, B.; Chiu, D. T. *Anal. Chem.* **2005**, *77*, 2770–2776.
(18) Lohse, B.; Bolinger, P.-Y.; Stamou, D. *J. Am. Chem. Soc.* **2008**, *130*, 14372–14373.
(19) Okumus, B.; Arslan, S.; Fengler, S. M.; Myong, S.; Ha, T. *J. Am. Chem. Soc.* **2009**, *131*, 14844–14849.
(20) Colletier, J.-P.; Chaize, B.; Winterhalter, M.; Fournier, D. *BMC Biotechnol.* **2002**, *2*, 9.
(21) MacDonald, R. C.; MacDonald, R. I.; Menco, B. P. M.; Takeshita, K.; Subbarao, N. K.; Hu, L.-r. *Biochim. Biophys. Acta* **1991**, *1061*, 297–303.
(22) Mayer, L. D.; Hope, M. J.; Cullis, P. R. *Biochim. Biophys. Acta* **1986**, *858*, 161–168.
(23) Barenholz, Y.; Gibbes, D.; Litman, B. J.; Goll, J.; Thomson, T. E.; Carlson, F. D. *Biochemistry* **1977**, *16*, 2806–2810.
(24) Castile, J. D.; Taylor, K. M. G. *Int. J. Pharm.* **1999**, *188*, 87–95.
(25) Reiner, J. E.; Jahn, A.; Stavis, S. M.; Culbertson, M. J.; Vreeland, W. N.; Burden, D. L.; Geist, J.; Gaitan, M. *Anal. Chem.* **2010**, *82*, 180–188.
(26) Chen, C.-S.; Yao, J.; Durst, R. *J. Nanopart. Res.* **2006**, *8*, 1033–1038.
(27) Rigler, P.; Meier, W. *J. Am. Chem. Soc.* **2005**, *128*, 367–373.
(28) Sackett, D. L.; Knutson, J. R.; Wolff, J. *J. Biol. Chem.* **1990**, *265*, 14899–14906.
(29) Gao, F.; Mei, E.; Lim, M.; Hochstrasser, R. M. *J. Am. Chem. Soc.* **2006**, *128*, 4814–4822.
(30) Johnson, J. M.; Ha, T.; Chu, S.; Boxer, S. G. *Biophys. J.* **2002**, *83*, 3371–3379.
(31) Peterson, E. M.; Harris, J. M. *Anal. Chem.* **2010**, 189–196.
(32) Hanley, D. C.; Harris, J. M. *Anal. Chem.* **2001**, *73*, 5030–5037.
(33) Heider, E. C.; Barhoum, M.; Peterson, E. M.; Schaefer, J.; Harris, J. M. *Appl. Spectrosc.* **2010**, *64*, 37–45.
(34) Thompson, R. E.; Larson, D. R.; Webb, W. W. *Biophys. J.* **2002**, *82*, 2775–2783.
(35) Bracewell, R. N. *The Fourier Transform and Its Applications*; McGraw-Hill: New York, 1986.
(36) Schönherr, H.; Johnson, J. M.; Lenz, P.; Frank, C. W.; Boxer, S. G. *Langmuir* **2004**, *20*, 11600–11606.
(37) Duzgunes, N.; Paiement, J.; Freeman, K. B.; Lopez-Straubinger, N. G.; Wilschut, J.; Papahadjopoulos, D. *Biochemistry* **1984**, *23*, 3486–3494.
(38) Barlow, R. *Statistics: A Guide to the Use of Statistical Methods in the Physical Sciences*; Wiley: Chichester, U.K., 1989.
(39) Mutch, S. A.; Fujimoto, B. S.; Kuyper, C. L.; Kuo, J. S.; Bajjalieh, S. M.; Chiu, D. T. *Biophys. J.* **2007**, *92*, 2926–2943.
(40) Mutch, S. A.; Kensel-Hammes, P.; Gadd, J. C.; Fujimoto, B. S.; Allen, R. W.; Schiro, P. G.; Lorenz, R. M.; Kuyper, C. L.; Kuo, J. S.; Bajjalieh, S. M.; Chiu, D. T. *J. Neurosci.* **2011**, *31*, 1461–1470.
(41) Yip, W.-T.; Hu, D.; Yu, J.; Bout, D. A. V.; Barbara, P. F. *J. Phys. Chem. A* **1998**, *102*, 7564–7575.
(42) Gensch, T.; Böhmer, M.; Aramendía, P. F. *J. Phys. Chem. A* **2005**, *109*, 6652–6658.
(43) Lu, H. P.; Xie, X. S. *Nature* **1997**, *385*, 143–146.
(44) Ambrose, W. P.; Goodwin, P. M.; Martin, J. C.; Keller, R. A. *Phys. Rev. Lett.* **1994**, *72*, 160–163.
(45) Issac, A.; Borczyskowski, C. v.; Cichos, F. *Phys. Rev. B* **2005**, *71*, 161302-1 - 161302-4.
(46) Lohr, C.; Kunding, A. H.; Bhatia, V. K.; Stamou, D. *Methods Enzymol.* **2009**, *465*, 143–160.
(47) Rust, M. J.; Bates, M.; Zhuang, X. *Nat. Methods* **2006**, *3*, 793–795.
(48) Sharonov, A.; Hochstrasser, R. M. *Proc. Natl. Acad. Sci. U.S.A.* **2006**, *103*, 18911–18916.